

Effect of equiaxial microplastic deformation before final annealing on T_c of liquid-quenched $\text{Bi}_{1.6}\text{Pb}_{0.4}\text{Sr}_2\text{Ca}_2\text{Cu}_{2.7}\text{Ti}_{0.3}\text{O}_x$ crystallized

Y. NISHI, T. AIDA*, K. NOZAKI*, K. SHIRAIISHI*, K. OGURI*

Department of Materials Science, Tokai University, 1117 Kitakaname, Hiratsuka, Kanagawa, 259-12, Japan

The influence of the treatment (equiaxial microplastic deformation and final annealing) on the T_c^0 value is studied for the liquid-quenched $\text{Bi}_{1.6}\text{Pb}_{0.4}\text{Sr}_2\text{Ca}_2\text{Cu}_{2.7}\text{Ti}_{0.3}\text{O}_x$ which is crystallized. The treatment increases the T_c^0 value. Based on results of X-ray diffraction and electrical resistivity, the T_c^0 change is discussed.

1. Introduction

Since the melting points of high- T_c Bi oxides are low, they are easy to melt and liquid-quench. The density of the liquid-quenched sample is apparently higher than that of the sintered sample, which may improve their superconducting performance [1, 2]. From an engineering point of view, it is important to know the influence of cold-working on the superconducting properties. Although the compressive elastic stress improves the superconducting performance [3, 4], the influence of the plastic deformation has not been studied precisely. We just develop the equiaxial microplastic deformation process. Thus effects of the treatment (equiaxial microplastic deformation and final annealing) on T_c is investigated for the liquid-quenched $\text{Bi}_{1.6}\text{Pb}_{0.4}\text{Sr}_2\text{Ca}_2\text{Cu}_{2.7}\text{Ti}_{0.3}\text{O}_x$ crystallized. Here, the Ti addition improves the ductility of the Bi oxide [5] and does not greatly decrease the T_c value [6].

2. Experimental procedure

Samples with nominal composition were prepared from high-purity powders of CuO (99.9 wt %), TiO_2 (99.9 wt %), Bi_2O_3 (99.99 wt %), PbO (99.9 wt %), SrCO_3 (99.9 wt %) and CaCO_3 (99.99 wt %). The powders were mixed and reacted in air at 1023 K for 6 h and then air-cooled. The reacted powders were resintered in air at 1073 K for 18 h and then air-cooled. After crushing, a pelletized tablet, 1 mm thick and 13 mm in diameter, was sintered at 1123 K for 12 h and then furnace cooled in air.

Liquid-quenched glassy foils were prepared from chips cut from the sintered tablets using a twin-type piston-anvil apparatus [7, 8]. The twin-type piston-anvil apparatus was constructed to quench the molten sample at the centre of a quartz tube. The sample was melted by an infrared light source and

then quenched. The Cu cylindrical block was moved by a piston to touch the sample. The speed of the piston was about 0.12 m s^{-1} . The liquid-quenched sample was annealed at 1123 K for 26 h in air and then furnace-cooled. The equiaxial plastic deformation (see Fig. 1) was performed at $9.8 \times 10^{-2} \text{ GPa}$ in the pressure (equiaxial stress) transport of stainless steel without fracture. Since the pressure transport is slightly deformed during the small amount of working, the sample is almost lapped. In addition, the large pressure is loaded by the work-hardened stainless steel. Thus the equiaxial plastic deformation is performed without fracture. The microplastic deformed sample was finally annealed at 1123 K for 2 h and then furnace-cooled.

The electrical resistivity was measured using a standard 4-probe technique and a Keithley 181 nanovoltmeter. The temperature was measured by an Au*Fe/chromel thermocouple attached to the specimen in a cryostat at equilibrium temperature. The offset T_c^0 of the transition is defined as the temperature where zero-resistivity is reached (below $10^{-9} \Omega \text{ m}$ at 10^3 A m^{-2} current density). The structure of the sample was examined by means of X-ray diffraction. The diffraction measurements were performed under a step scanning mode (CuK_α target, 40 kV, 50 mA, $0.01 \text{ deg step}^{-1}$, 10 s step^{-1}).

3. Results and discussion

3.1. T_c measurements

Fig. 2 shows the change in the electrical resistivity (R_c) against the temperature (T) of the annealed $\text{Bi}_{1.6}\text{Pb}_{0.4}\text{Sr}_2\text{Ca}_2\text{Cu}_{2.7}\text{Ti}_{0.3}\text{O}_x$ sample with and without the treatment (equiaxial microplastic deformation and final annealing). The offset temperatures (T_c^0) of the samples with and without the treatment are 98.9 K and 93.7 K, respectively. The

* Student of Materials Science, Tokai University.

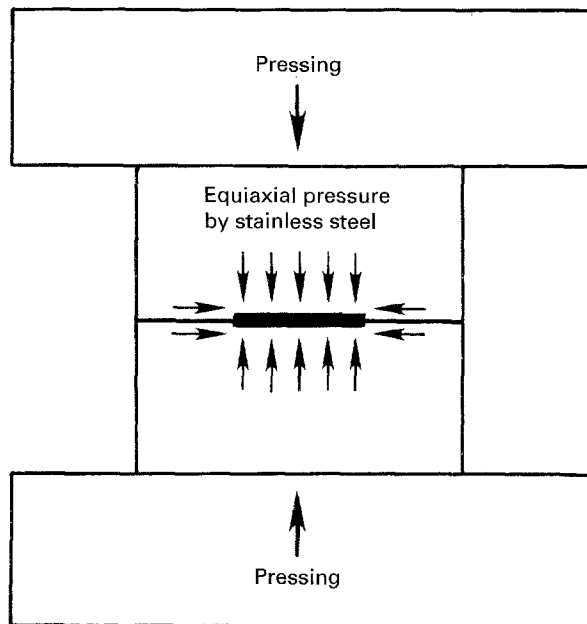


Figure 1 Schematic apparatus for equiaxial microplastic deformation.

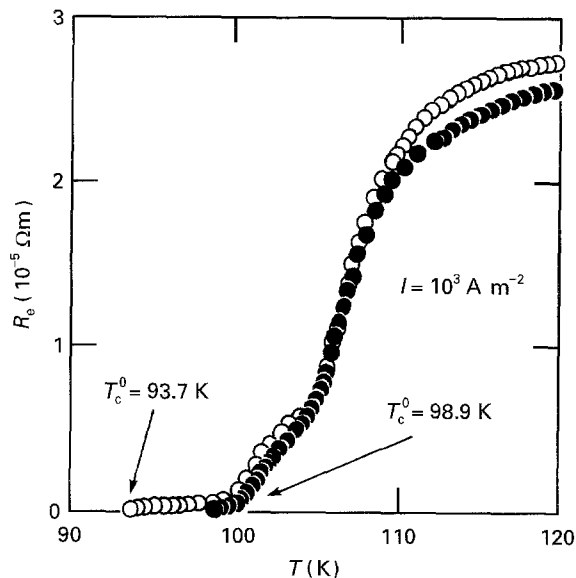


Figure 2 Change in electrical resistivity (R_e) against temperature (T) of $\text{Bi}_{1.6}\text{Pb}_{0.4}\text{Sr}_2\text{Ca}_2\text{Cu}_{2.7}\text{Ti}_{0.3}\text{O}_x$ sample with (●) and without (○) treatment (equiaxial microplastic deformation and final annealing).

T_c^0 increasing is 5.2 K by the treatment. On the other hand, a superconducting transition is not observed on the deformed sample without the final annealing.

The value of the T_c^0 depends on measuring current density (I). Fig. 3 shows the change in the T_c^0 value against the electrical current densities (I) of the annealed bulk sample with and without the treatment (equiaxial microplastic deformation and final annealing). The solid and dotted lines are for the samples with and without the treatments, respectively. The T_c^0 value increases with decreasing I . Fig. 4 shows the T_c^0 change against number of treatment (equiaxial microplastic deformation and final annealing). The treatments apparently improve the T_c^0 value. The maximum T_c^0 values are found at the first treatment.

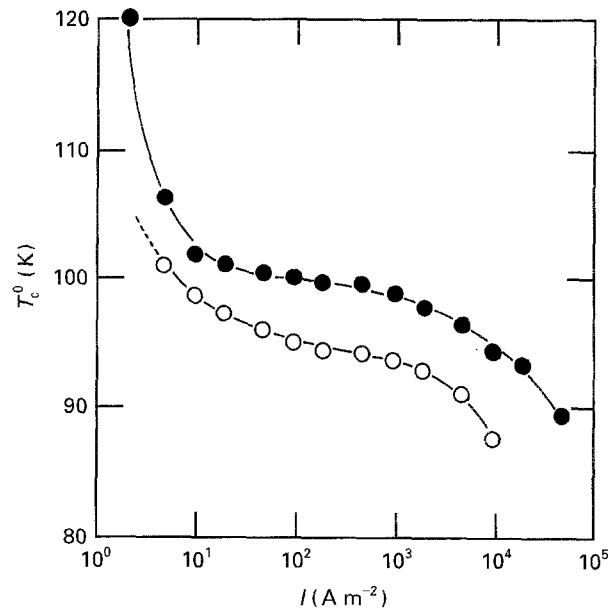


Figure 3 Change in T_c^0 against current density (I) of $\text{Bi}_{1.6}\text{Pb}_{0.4}\text{Sr}_2\text{Ca}_2\text{Cu}_{2.7}\text{Ti}_{0.3}\text{O}_x$ sample with (●) and without (○) treatment (equiaxial microplastic deformation and final annealing).

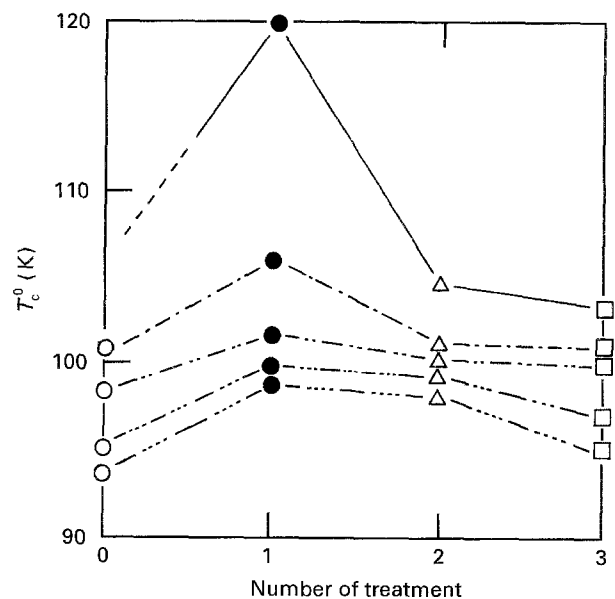


Figure 4 Changes in offset temperature (T_c^0) of superconducting transition temperature at different current densities (2 (—), 5 (---), 10 (·····), 10^2 (-·-·-·), and 10^3 (- - - - -), A m^{-2}) against number of treatment (equiaxial microplastic deformation and final annealing) for $\text{Bi}_{1.6}\text{Pb}_{0.4}\text{Sr}_2\text{Ca}_2\text{Cu}_{2.7}\text{Ti}_{0.3}\text{O}_x$.

The effect of the first treatment on the T_c^0 value is remarkable at the small I values. We found the highest T_c^0 value (120 K) at 2 A m^{-2} (see Figs 3 and 4).

3.2. X-ray diffraction

Fig. 5 shows the X-ray diffraction peaks of the (002) plane of the $\text{Bi}_{1.6}\text{Pb}_{0.4}\text{Sr}_2\text{Ca}_2\text{Cu}_{2.7}\text{Ti}_{0.3}\text{O}_x$. The samples are mixtures of the high- T_c (triple Cu-O layer) and low- T_c (double Cu-O layer) phases [9, 10]. Since the crystal orientation affects the peak height of the bulk samples, the volume fraction of the high- T_c (2223) and the low- T_c (2212) phases should be

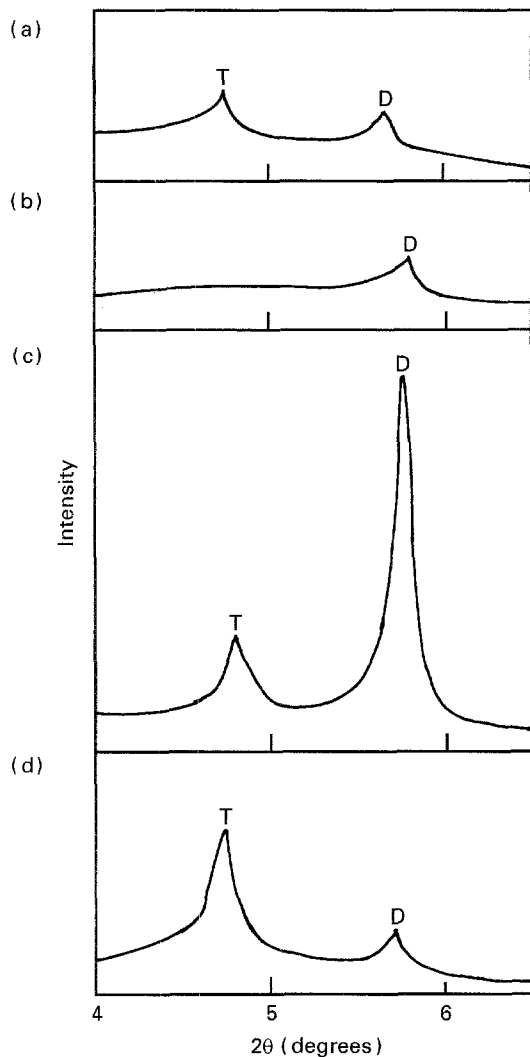


Figure 5 X-ray diffraction peaks of (002) plane of $\text{Bi}_{1.6}\text{Pb}_{0.4}\text{Sr}_2\text{Ca}_2\text{Cu}_{2.7}\text{Ti}_{0.3}\text{O}_x$: (a) annealed powdered sample before the first treatment; (b) annealed bulk sample before the first treatment; (c) bulk sample after the first microplastic deformation; (d) bulk sample after the first treatment (equiaxial microplastic deformation and final annealing). T, high T_c phase (2223); D, low T_c phase (2212).

deduced from the peak heights for the powdered sample (see Fig. 5(a)). On the other hand, the internal stress, which largely affects the T_c value, is usually obtained by the X-ray diffraction results of the bulk sample. A high- T_c peak cannot be found for the annealed bulk sample (see Fig. 5(b)). Although a T_c value above 4.2 K cannot be found for the powdered and the plastic deformed samples, the high- T_c peaks of the (2223) phase can be found (see Fig. 5(a), (c)). The large high- T_c peak (see Fig. 5(d)) is found for the first treated (microplastic deformed and finally annealed) sample which shows the highest T_c value (see Figs 3 and 4). The first treatment (microplastic deformation and final annealing) generates the large peak height of the high- T_c (2223) phase and induces the high- T_c value.

Fig. 6 shows the change in the lattice constant of the (002) peak for the high- T_c phase against number of the treatment (microplastic deformation and final annealing). The annealed bulk samples usually have internal stress among the ions, because the X-ray

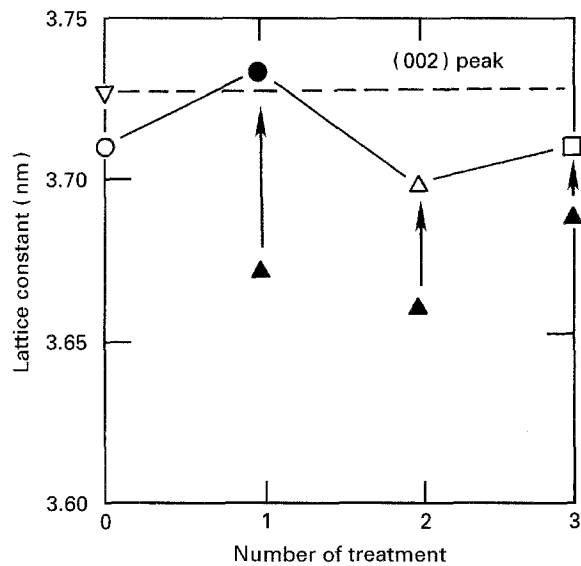


Figure 6 Changes in lattice constant against number of treatment (equiaxial microplastic deformation and final annealing) of (002) peak of $\text{Bi}_{1.6}\text{Pb}_{0.4}\text{Sr}_2\text{Ca}_2\text{Cu}_{2.7}\text{Ti}_{0.3}\text{O}_x$ sample. Broken line is for powdered sample. \circ bulk sample before treatment; \blacktriangle bulk sample after deformation; \square bulk sample after treatment; ∇ powdered sample before treatment.

peaks are broad (see Fig. 5(b)). On the other hand, the powdered sample has sharp peaks (see Fig. 5(a)). It shows that internal stress is relaxed among the ions. Since the sample of fine particles has a broad area of grain boundary, it is easy for the dislocation to annihilate to the surface by the image force [11]. The density of the dislocation is often low in the film sample [12]. Thus the powdered $\text{Bi}_{1.6}\text{Pb}_{0.4}\text{Sr}_2\text{Ca}_2\text{Cu}_{2.7}\text{Ti}_{0.3}\text{O}_x$ sample is likely to be stress-free whereas a small amount of internal stress exists in the bulk samples.

The lattice constant of the first treatment is approximately equal to that of the powdered sample. It shows that the first treatment largely relaxes the residual stress in the bulk $\text{Bi}_{1.6}\text{Pb}_{0.4}\text{Sr}_2\text{Ca}_2\text{Cu}_{2.7}\text{Ti}_{0.3}\text{O}_x$ sample. The abnormal rapid growth of the recrystallization is often induced by the small strain (about 5%) in alloys [13]. The small strain increases the defect density and the defects improve the atom diffusivity. In addition, the nucleation sites are formed by the defects, although the number of the sites is small. Thus they improve the abnormal rapid growth of the recrystallization. Since the crystal perfection is generally high in the easily recrystallized materials, the first treatment largely relaxes the residual stress in the bulk $\text{Bi}_{1.6}\text{Pb}_{0.4}\text{Sr}_2\text{Ca}_2\text{Cu}_{2.7}\text{Ti}_{0.3}\text{O}_x$ sample. Therefore, a high- T_c can be found with the first treatment. It is notable that the small superconducting current can pass through the small amount of defect-free zone. Thus, the high- T_c above 120 K is probably found at 2 A m^{-2} of the small I value.

On the other hand, the large strain generates excess defects. They induce excess nucleation sites of the recrystallization and retain the stable defects. Stable defects are often found for gold [14, 15] and the high- T_c Bi oxide recrystallized [16]. Thus, the second and third treatments retain the crystal imperfection.

Since the crystal imperfection is usually found in the excess-treated sample, the second and third treatments decrease the T_c value.

3.3. Discussion of electronic properties

A carrier concentration (C^*) is one of the dominant factors to control the T_c . C^* can be expressed by the following equation [17, 18]

$$C^* = N [\exp(\pm eO/k - A)]^{-1} \quad (1)$$

where, N , Q , k , e and A are density of state, Seebeck coefficient, Boltzmann constant, electron charge and constant, respectively. Since the band gaps for the high- T_c oxides are smaller than those of semiconductors, A is assumed to be about zero [17, 18]. Thus, N and Q affect C^* . Since the Q value of the high- T_c Bi system are approximately zero, an exponential term of the sample is about 1 [19]. Thus, C^* is dominated by the density of state (N). N can be estimated using the electrical resistivity (R_e). N is usually expressed by the following equation [20]

$$N = A'R_e^{-1/2} \quad (2)$$

Here, A' is constant, which is dominated by the electron mass, the charge, Planck's constant and mean free path. If we assume that the treatment (equiaxial microplastic deformation and final annealing) does not largely change the mean free path, the N value is inversely proportional to the $R_e^{1/2}$ value. Fig. 7 shows the change in the reciprocal square root of electrical

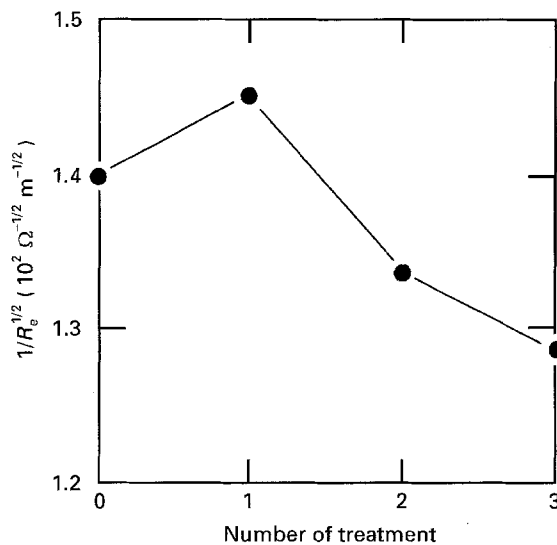


Figure 7 Change in reciprocal square root of electrical resistivity ($1/R_e^{1/2}$) at 300 K against number of treatment (equiaxial microplastic deformation and final annealing) for $\text{Bi}_{1.6}\text{Pb}_{0.4}\text{Sr}_2\text{Ca}_2\text{Cu}_{2.7}\text{Ti}_{0.3}\text{O}_x$.

resistivity ($1/R_e^{1/2}$) at 300 K against the number of treatments (equiaxial microplastic deformation and final annealing) for the $\text{Bi}_{1.6}\text{Pb}_{0.4}\text{Sr}_2\text{Ca}_2\text{Cu}_{2.7}\text{Ti}_{0.3}\text{O}_x$. The change in the $1/R_e^{1/2}$ values (see Fig. 7) approximately agrees with the change in the T_c^0 values (see Fig. 4).

4. Conclusion

In summary, the effect of the treatment (equiaxial microplastic deformation and final annealing) on the T_c value is investigated for the liquid-quenched $\text{Bi}_{1.6}\text{Pb}_{0.4}\text{Sr}_2\text{Ca}_2\text{Cu}_{2.7}\text{Ti}_{0.3}\text{O}_x$ which is crystallized. The treatment increases the T_c^0 value. The high- T_c sample shows low electrical resistivity (the high density of states and high carrier concentration) and sharp (002) diffraction peaks (the high crystal perfection of the triple Cu-O layer phase).

References

1. Y. NISHI, S. MORIYA and T. MANABE, *J. Appl. Phys.* **65** (1989) 2389.
2. Y. NISHI, Y. KITA and K. TANIOKA, *J. Mater. Sci.* **25** (1990) 5105.
3. T. ASAKA, Y. OKAZAWA, T. HIRAYAMA, and K. TACHIKAWA, *Jpn. J. Appl. Phys.* **29** (1990) 280.
4. T. ASAKA, Y. OKAZAWA and K. TACHIKAWA, *J. Jpn. Inst. Matl.* **56** (1992) 715.
5. K. NOZAKI, K. SHIRAIISHI, S. UCHIDA, M. SHIMABARA and Y. NISHI, *Trans. Mater. Res. Soc. Jpn.*, **19A** (1993) 475.
6. Y. NISHI, K. NOZAKI and T. KUROTAKE, *J. Appl. Phys.* **71** (1992) 350.
7. Y. NISHI, T. KAI and K. KITAGO, *Wear* **126** (1988) 191.
8. Y. NISHI and H. HARANO, *J. Appl. Phys.* **63** (1988) 1141.
9. H. NOBUMASA, K. SHIMIZU, Y. KITANO and T. KAWAI, *Jpn. J. Appl. Phys.* **27** (1988) L846.
10. H. NOBUMASA, K. SHIMIZU, Y. KITANO and T. KAWAI, *Ibid.* **27** (1988) L1669.
11. A. K. HEAD, *Proc. Phys. Soc. Lond. B* **66** (1953) 793.
12. S. MADER, A. SEEGER and H. M. THIERINGER, *J. Appl. Phys.* **34** (1963) 3376.
13. F. BOURELIER, *Mem. Sci. Rev. Met.* **65** (1968) 34.
14. J. SILCOX and P. B. HIRSCH, *Phil. Mag.* **4** (1959) 72.
15. R. M. J. COTTERILL, *Ibid.* **6** (1961) 1351.
16. S. IKEDA, H. ICHINOSE, T. KIMURA, T. MATSUMOTO, H. MAEDA and K. OGAWA, *Jpn. J. Appl. Phys.* **27** (1988) L999.
17. N. M. TALLAN and I. BRANSKY, *J. Electrochem. Soc.* **118** (1971) 345.
18. R. F. BREBRICK, in "Defects in solids", Vol. 2 of "Treatise on solid state chemistry", edited by N. B. Hannay (Plenum Press, New York, 1975), p. 357.
19. Y. NISHI, K. OGURI, H. OHINATA, K. TANIOKA, Y. KITA and N. NINOMIYA, *Phys. Rev. B* **41** (1990) 6520.
20. N. F. MOTT, *Phil. Mag.* **19** (1969) 835.

Received 3 December 1993

and accepted 3 February 1995